Journal of Mining and Earth Sciences

Website: http://tapchi.humg.edu.vn

Comparison of the resampling methods for gridded dem downscaling

Huong Thu Thi Nguyen [1], Minh Quang Nguyen [2,*], Hien Phu La [2]

[1] *Faculty of Geomatics and Land Administration, Hanoi University of Mining and Geology, Vietnam*
[2] *Thuy Loi University, Vietnam*

ARTICLE INFO

Article history:
Received 3rd June. 2018
Accepted 18th Nov. 2018
Available online 31st Dec 2018

Keywords:
Resampling
Kriging
DEM
Interpolation

ABSTRACT

In this paper, a comparison and evaluation of three resampling methods for gridded DEM is implemented. The evaluation was based on the results of bilinear, bi-cubic and Kriging resampling methods for an experiment using both degraded and sampled datasets at 20 m, 60 m and 90 m spatial resolutions. The evaluation of the algorithms was accomplished comprehensively with visual and quantitative assessments. The visual assessment process was based on direct comparison of the same topographic features in different resampled images, scatter plots and profiles. The quantitative assessment was based on the most commonly used parameters for DEM accuracy assessment such as root mean square errors (RMSEs), linear regression parameters m and b, and correlation coefficient R of the resulted DEMs versus the reference DEM. Both visual and quantitative assessment revealed a greater accuracy of the Kriging resampling over the other two conventional methods with the RMSE of the Kriging interpolated DEMs decreased by approximately 58%, 23%, 50%, and 58% for the 20 m and 30 m degraded DEMs in Nghe An province, 5 m sampled DEM in Lang son province, and 30 m sampled DEM in Dac Ha, Vietnam, respectively.

1. Introduction

The spatial resolution of a gridded DEM affects both the information content and the accuracy of the data and, potentially, of many other secondary data products (Reddy and Reddy, 2015; Saksena and Merwade, 2015). Examples include the well-known effects of spatial resolution on the spatial properties of DEM and other spatial data (Bian and Butler, 1999; Zhao et al., 2010) such as specifically on slope and aspect (Bolstad, Paul V. & Stowe, 1994; Chang and Tsai, 2008), watershed boundary delineation and the accuracy of SWAT schemes (Chaubey et al., 2005; Rawat et al., 2018), water run-off models (Vázquez and Feyen, 2007; Vieux, 2006), three dimensional modelling of landscapes (Schoorl et al., 2000), local slope, plan curvature, drainage area (Li and Wong, 2010; Sulis et al., 2011),

*Corresponding author
E-mail: nguyenquangminh@humg.edu.vn

soil survey results and soil moisture (Kuo et al., 1999; Smith et al., 2006).These studies showed that DEMs with a finer spatial resolution can produce more informative and potentially more accurate data to many other applications.

Gridded DEMs with fine spatial resolution and high accuracy can be acquired using airborne LiDAR technology, ground surveying and photogrammetry(Guo et al., 2013; Wilson, 2012). Airborne LiDAR enables the acquisition of data with a very accurate and high density of 3-dimensional coordinate points and, therefore, the production of a DEM with sub-meter spatial resolution. Airborne LiDAR-derived DEMs have been used in many different applications, some of which require very fine spatial resolution and very high accuracy (Rapinel et al., 2015). Although being capable of generating a fine spatial resolution DEM, airborne LiDAR technology has some challenges such as the very large amount of data storage required and high computing capacity for data processing. Compared with airborne LiDAR, other methods for fine spatial resolution DEM acquisition such as ground surveying and photogrammetry are more time consuming and labour intensive (Liu, 2008). Hence, if the resolution of the DEM can be increased using algorithms, it is possible to save the time and labour cost.

Sometimes, it is necessary to resample the raster DEM to a higher resolution using the common algorithms such as nearest neighbour, bilinear and bi-cubic interpolation. Potentially, these algorithms can downscale the raster DEM data (Kidner et al., 1999). That means the resolution or the accuracy of raster DEM were slightly improved through resampling using these approaches (Shi et al., 2014; Wu et al., 2008). Another method for resampling gridded DEM data to a finer resolution with higher accuracy is Kriging interpolation (Grohmann and Steiner, 2008). To test the ability of increasing the resolution and accuracy of the resampling algorithms, Dixon and Earls (Dixon and Earls, 2009) used the simple nearest neighbour resampling to increase the resolution of DEMs and compare the effects of results to the DEM's products such as stream flow, watershed, delineations, number of sub-basins and slopes. It was showed that the simple resampling of DEM did not increase the accuracy of DEMs greatly, or, the resampling methods did not create new significant information that is not available at the original resolution of DEM (Band and Moore, 1995). The experiments by Rees (Rees, 2000) and Shi et. al. (Shi et al., 2014) showed that bilinear, bicubic and Kriging resampling increased the accuracy of DEMs in term of root mean square error (RMSE) with a suitable value of resampling ratio r. Comparing three resampling methods, Kriging performed better than the other two methods for smooth terrain. However, for terrain with high roughness, the performance of three resampling were similar (Rees, 2000). All of researches suggested that the resampling of raster DEM data can potentially increase the spatial resolution of the data and it is necessary to have further evaluation on the ability of increasing spatial resolution of these algorithms. For that reason, in this paper, the comprehensive evaluation of the algorithms was accomplished with new visual and quantitative parameters. The visual assessment process was based on direct comparison of the same topographic features in different downscaled images, scatterplots and profiles. The quantitative assessment was based on the most commonly used parameters for DEM accuracy assessment such as root mean square errors (RMSEs), linear regression parameters m and b, and correlation coefficient *R*.

2. Method

2.1. Bilinear resampling

Suppose that the value of the unknown function f at the point (x, y), for example the elevation of the point (x, y). It is assumed that we know the value of f at the four points $Q_{11} = (x_1, y_1)$, $Q_{12} = (x_1, y_2)$, $Q_{21} = (x_2, y_1)$, and $Q_{22} = (x_2, y_2)$ (Fadnavis, 2014) Figure 1.

The value of point (x, y) is estimated as:

$$f(x,y) = \frac{1}{(x_2 - x_1)(y_2 - y_1)} \quad (1)$$
$$[x_2 - x \quad x - x_1] \begin{bmatrix} f(Q_{11}) & f(Q_{11}) \\ f(Q_{11}) & f(Q_{11}) \end{bmatrix} \begin{bmatrix} y_2 - y \\ y - y_1 \end{bmatrix}$$

2.2. Bi-cubic resampling

Different to the bilinear resampling, the value of unknown function f at the point (x, y), for

example the elevation of the point (x, y), is calculated from 16 adjacent data points. The calculation is more complicated, and the data value of the point is affected not by the only closest data points. Figure 2**Error! Reference source not found.** shows how the data value of the points is estimated using 16 surrounding

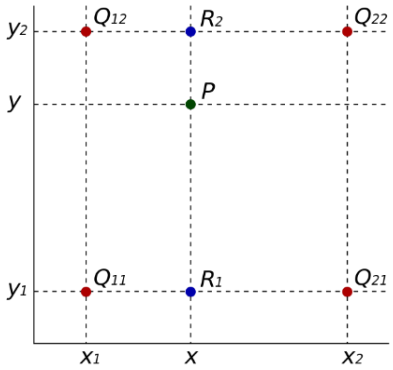

Figure 1. Bilinear resampling to estimate the value f of the point P(x, y) from the point Q_{11} = (x_1, y_1), Q_{12} = (x_1, y_2), Q_{21} = (x_2, y_1), and Q_{22} = (x_2, y_2).

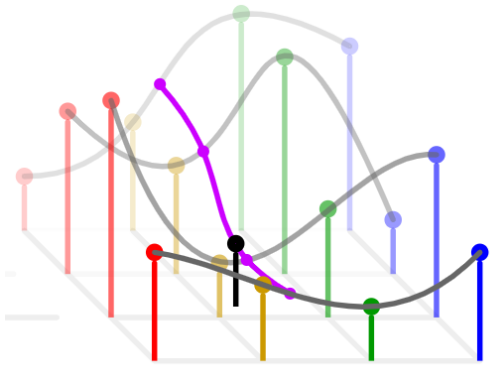

Figure 2. Bi-cubic calculation of the data point from surrounding 16 points.

points (Fadnavis, 2014).

2.3. Kriging interpolation

The basic idea of Kriging is to predict the value of a function at a given point by computing a weighted average of the known values of the function in the neighbourhood of the point (Fadnavis, 2014). The method is mathematically closely related to regression analysis. Kriging aims to derive a best linear unbiased estimator, based on assumptions on covariances, make use of Gauss-Markov theorem to prove independence of the estimate and error, and make use of very similar formulae. Kriging is based on the semivariogram value as

$$\gamma(h) = \frac{1}{2N(h)} \sum_{1}^{N(h)} \left[Z(x_i) - Z(x_j) \right]^2 \quad (2)$$

Where $\gamma(h)$ is variogram value, N is number of sample data points, h is distance between two data points, $Z(x_i)$ and $Z(x_j)$ is data value of point x_i and x_j, respectively.

The semivariogam is firstly estimated from the sample data points and then used to estimate the data value of the predicted point based as follows:

$$Z(x_0) = \sum_{1}^{n} w_i(x_0)\, Z(x_i) \quad (3)$$

Where $w_i(x_0)$ is weight value which is calculated using semivariogram.

2.4. Method of assessment

To test these three algorithms for resampling, the DEMs with coarser spatial resolution were used as an input to the resampling algorithms to produce DEMs at the same resolution of reference data using the bilinear, bi-cubic resampling, and Kriging interpolation. Because the accuracy of Kriging interpolation is contingent on the selection of the parameters, in this experiment, several Kriging parameters such as semivariogam model, number of samples and range of searching for samples were tested to find the best parameters. The most accurate results were selected with Kriging interpolation using exponential variogram model with 8 samples. Results of these resampling for four datasets are presented in Figure 3, Figure 4, Figure 5, Figure 6.

The assessment was implemented based on both visual comparison of the resulting DEMs from the three different methods using visual inspection, and the comparison of scatterplots and profiles. The quantitative evaluation was based on the parameters which were usually used for DEMs' accuracy assessment such as RMSE (Alganci et al., 2018), coefficient of determination, linear regression parameters, and the elevation profiles (Kienzle, 2003).

Visual assessment of the results was carried out by several approaches. The first approach is

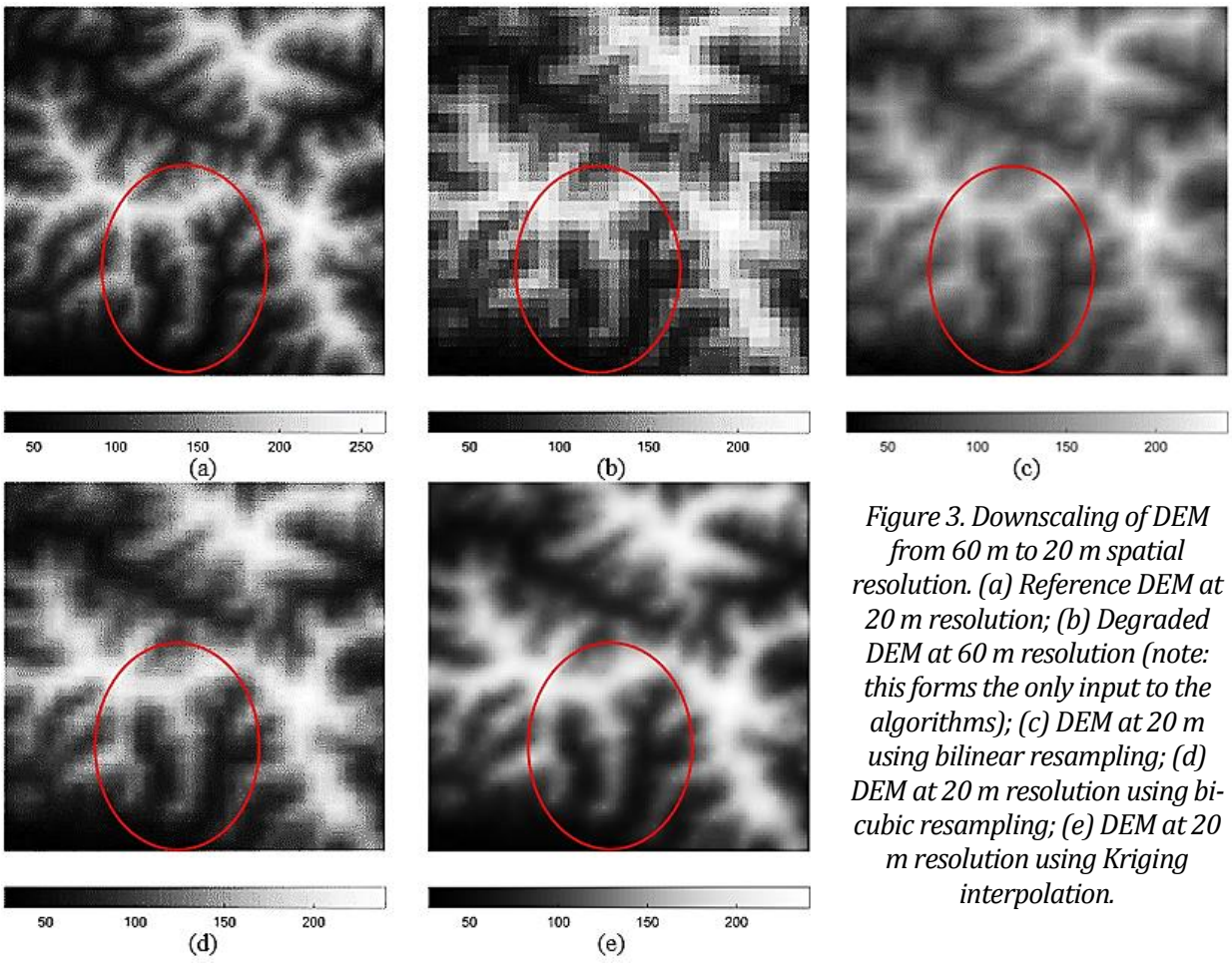

Figure 3. Downscaling of DEM from 60 m to 20 m spatial resolution. (a) Reference DEM at 20 m resolution; (b) Degraded DEM at 60 m resolution (note: this forms the only input to the algorithms); (c) DEM at 20 m using bilinear resampling; (d) DEM at 20 m resolution using bi-cubic resampling; (e) DEM at 20 m resolution using Kriging interpolation.

direct visual comparison of the DEM images, especially comparison of the images of same topographical features in different images. The second approach is to analyse the scatterplots between the elevation values the pixels of reference DEMs and the elevation values of the corresponding pixels of the bilinear and bi-cubic resampled DEMs, and Kriging interpolated DEM as in Figure 9, Figure10, Figure11, Figure 12. Another approach which was used in many previous research on DEMs evaluation is comparing the cross-sections (profiles) of the resulted downscaled DEMs (Alganci et al., 2018; Kienzle, 2003). These profiles present the match between the surfaces formed by the reference fine spatial resolution DEM and the surfaces formed by DEM at coarse spatial resolution, DEMs generated by bilinear, bi-cubic resampling, and Kriging interpolation algorithms and therefore enable the evaluation of the effects of the algorithms on different forms of terrain and topographical features. The locations of the profiles for the four datasets are presented in Figure 8.

The quantitative assessment was implemented mainly based on the RMSEs for whole images and profiles of the Nghe An (20 m spatial resolution and 30 m spatial resolution), Lang Son and Dac Ha datasets as presented in Table 2, Table 3, Table 4 and Table 5, respectively. Together with the RMSEs, the linear regression was implemented between the reference DEM and resampled DEMs. The evaluation was then based on linear regression coefficients such as slope m, intercept b, and correlation R to assess the match between the downscaled DEMs from the bilinear and bi-cubic resampling methods, Kriging interpolation and the reference DEMs for 4 datasets as in Table 6.

3. Reference and testing data

Two types of data were used to evaluate the proposed algorithm. The first type of data was

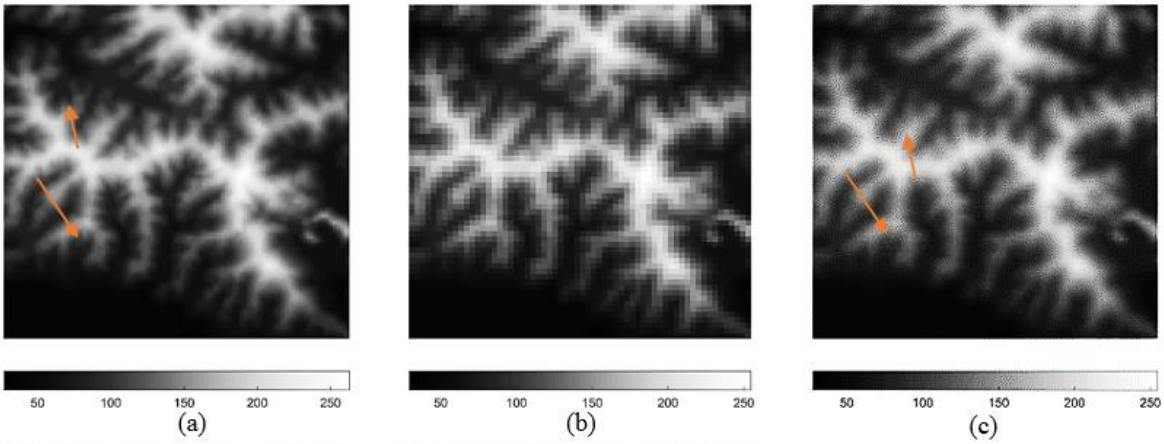

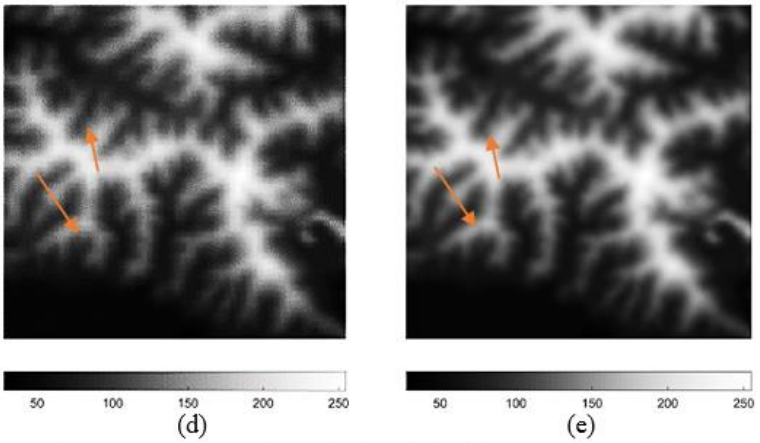

Figure 2. Downscaling of DEM from 90 m to 30 m spatial resolution. (a) Reference DEM at 30 m resolution; (b) Degraded DEM at 90 m resolution (note: this forms the only input to the algorithms); (c) DEM at 30 m resolution resulted from bilinear resampling; (d) DEM 30 m resolution resulted from bi-cubic resampling; (e) DEM at 30 m resolution resulted by Kriging interpolation.

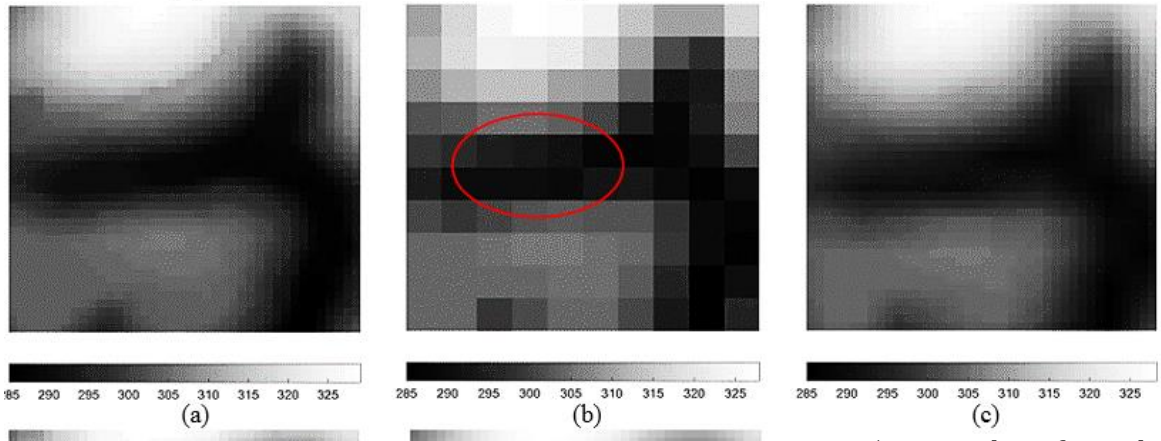

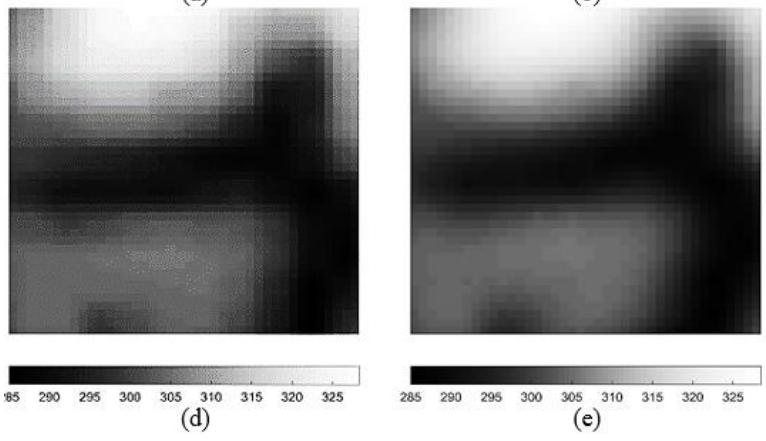

Figure 5 Downscaling of DEM data from 20 m to 5 m spatial resolution. (a) Reference DEM data at 5 m resolution; (b) Degraded DEM data at 20 m resolution (note: this forms the only input to the algorithms); (c) DEM at 5 m resolution resulted from bilinear resampling; (d) DEM at 5 m resolution resulted from bi-cubic resampling; (e) DEM at 5 m resolution resulted from Kriging interpolation.

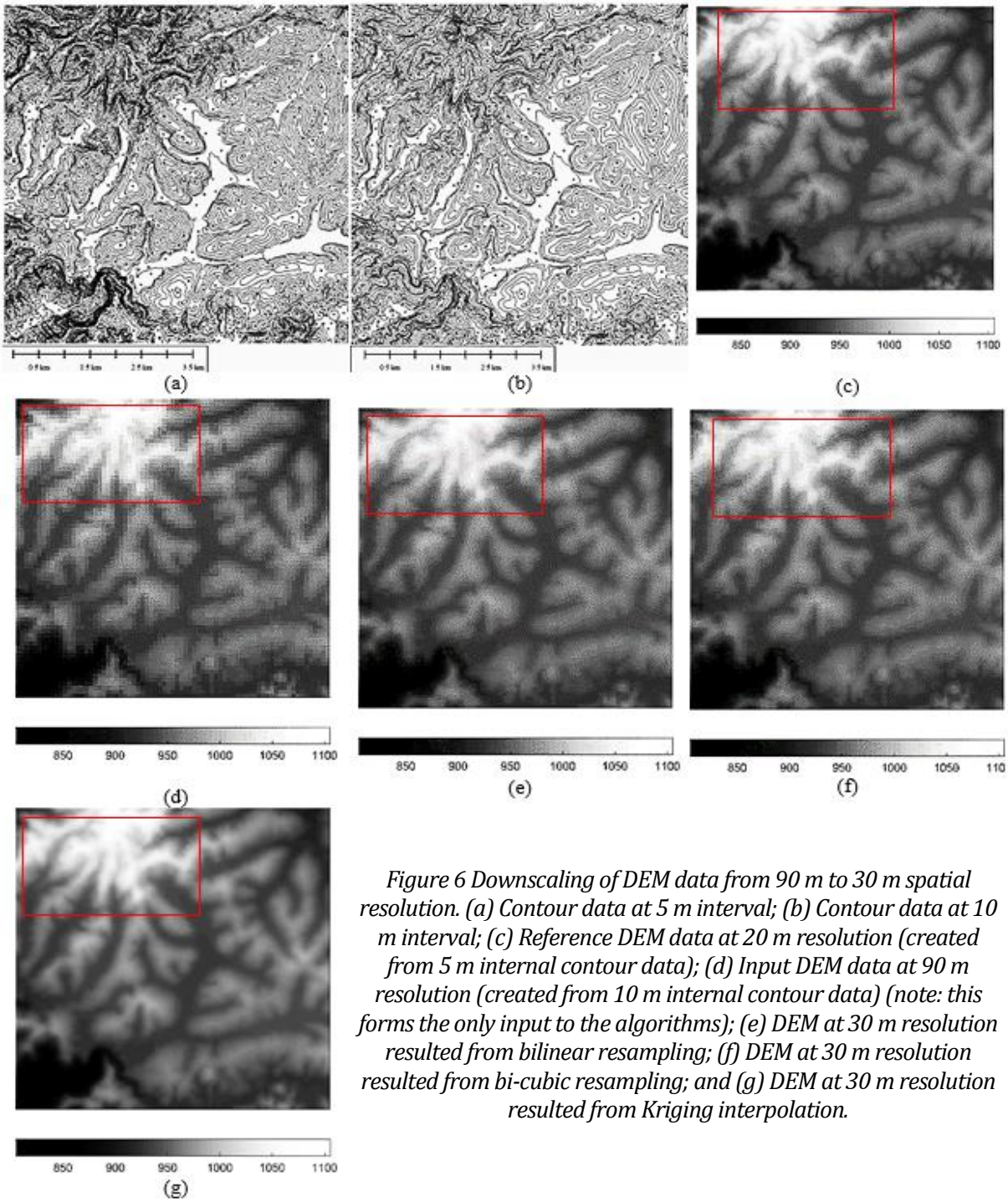

Figure 6 Downscaling of DEM data from 90 m to 30 m spatial resolution. (a) Contour data at 5 m interval; (b) Contour data at 10 m interval; (c) Reference DEM data at 20 m resolution (created from 5 m internal contour data); (d) Input DEM data at 90 m resolution (created from 10 m internal contour data) (note: this forms the only input to the algorithms); (e) DEM at 30 m resolution resulted from bilinear resampling; (f) DEM at 30 m resolution resulted from bi-cubic resampling; and (g) DEM at 30 m resolution resulted from Kriging interpolation.

degraded coarse DEMs which were calculated from the reference DEMs at fine resolution using nearest neighbour (or averaging method) to make a source of error-free data for algorithm testing. Error-free in this case means the elevation values of pixels in DEM do not contain interpolation and measurement errors. The difference between these degraded and reference DEM was due to the difference in the resolution only. These data alone may be enough to assess the algorithms' performance but it may lead to a scepticism because they were not real DEMs. The real DEMs are mostly sampled from point elevation or contour data rather than being averaged from the

elevation of sub-pixels within a footprint of the original pixel. Actually, the elevation of a pixel of the DEM represents the elevation of the surface area covered by this pixel so it must be the averaged elevation of all point of that surface area. The interpolation algorithms are used to estimate this representing elevation from point or contour data so the elevation of a pixel in the real grid DEMs is actually the averaged elevation of all points within the footprint of this pixel with some estimation errors. To implement more comprehensive evaluation of the algorithms, the *sampled (real)* DEMs generated by interpolating point elevation and contour data were used.

Table 1. Accuracy assessment based on ASPRS accuracy standard for digital geospatial data.

Dataset and standards	Absolute Accuracy			Appropriate Contour Interval Supported by the RMSEz value
	$RMSE_z$ Non-Vegetated (m)	NVA at 95% Confidence Level (cm)	VVA at 95th Percentile (cm)	
Mai Pha, Langson DEM	0.483	1.449-meter	1.449	1.449-meter
Standard ASPRS class VIII (66.7-cm)	0.667	2-meter	200	2-meter

The spatial resolution for all four testing DEM datasets in this paper was selected between 5 m and 90 m and, accordingly, the zoom factor values are 3 or 4. There are two reasons for this selection the spatial resolution. The first reason is because most of currently available sources of grid DEM data are at this range of resolution. The second about 150 km from Hanoi. A set of 533 measured elevation points were used with Kriging interpolation to generate a gridded DEM dataset at 5 m spatial resolution for use as a reference, as can be seen in Figure 5(a). The accuracy of reference DEM was assessed based on the ASPRS Accuracy Standard for Digital Geospatial Data with a set of 234 validation points. The results of assessment (Table 1) showed that the quality of the reference DEM is slightly better than that of 66.7-cm ASPRS DEM Class and Class VIII of ASPRS 1990 Standards (ASPRS, 2015; Whitehead and Hugenholtz, 2015) with RMSEz of 48.3 cm and the Appropriate Contour interval of 1.449-meter. The coarse DEM at 20 m spatial resolution was created using the same interpolation algorithm from the point data (Figure 5(b)). This coarse 20 m DEM was used as input for the algorithms to make 5 m DEM and this result was compared with 5 m DEM reference data.

The second sampled DEM dataset (named as S2 dataset) was created from contour data in and more important reason is that the increasing in accuracy of the data at these spatial resolutions is useful for many applications.

Finer resolution grid DEM data may be obtained from airborne LiDAR or 3D Laser scanners but they are accurate for most applications therefore increasing in accuracy or resolution of these types of data are actually not necessary and meaningful.

3.1. Degraded DEMs

The first set of degraded DEM data covered an area of about 3.5 km by 3.5 km and were acquired at Yen Thanh District, NgheAn Province, in North Central Vietnam. The area is located at 18°58'57.03" N, 105°22' 44.87" E, about 45 km from Vinh City. This DEM was produced from topographic maps at the scale of 1:10000. The spatial resolution of the original DEM is 20 m (Figure 3(a)) and this was degraded to 60 m by averaging the elevation value of 20 m pixels within the footprint of the degraded 60 m Figure 3(b)).

The second degraded DEM dataset was provided by the Shuttle Radar Topography Mission (SRTM) of the USGS Earth Explorer (http://earthexplorer.usgs.gov/) (Figure 4(a)). This dataset covered the same area as the first DEM but with a spatial resolution of 30 m. This was also degraded to 90 m to create a second set of test data for the resampling algorithms (Figure 4(b)).

3.2. Sampled DEMs

The first sampled dataset was acquired using ground surveying in Lang Son Province of Vietnam. The area of the test field is about 200 m by 200 m in Mai Pha Ward, Lang Son City which is

Dac Ha district in Kontum Province in Vietnam. The location of this DEM dataset was at 14.671794° N and 107.967292° E. The area of the test field is about 6.6 km by 6.6 km. From the original contour data at 5 m interval (Figure 6(a)), a 30 m resolution DEMs were generated and used as reference data (Figure 6(c)). The coarse 90 m spatial resolution data (Figure 6(d)) was then interpolated from the 10 m interval contours of the same area (Figure 6(b)). The evaluation is then implemented by comparing the resulted 30 m DEMs which were downscaled from coarse 90 m DEMs (zoom factor of 3) with reference data.

4. Visual assessment

Visual comparison showed that the resulting DEMs generated by the bilinear and bi-cubic resampling methods, and Kriging interpolation are visually more similar to the reference DEM than the coarse spatial resolution DEMs for both degraded and sampled datasets. The improvement in visual similarity between the resampled DEMs and reference DEM is seen clearly when comparing between the 20 m and 30 m DEMs in degraded datasets in Nghe An (Figure 3 and Figure 4) and 5 m and 30 m DEMs resampled datasets with reference DEMs (Figure 5 and Figure 6). While the images of original coarse resolution DEMs and the DEMs by resampling and methods, especially the images created by bi-cubic resampling, were blurred with noises and the shapes of terrain features in these images look distorted, the images of Kriging interpolation downscaled DEMs in Figure 3(e), Figure 4(e), Figure 5(e) and Figure 6(g) look noise-free and very similar to the reference DEMs in Figure 3(a), Figure 4(a), Figure 5(a), and Figure 6(c). The most clearly improvement of reconstruction of the shapes of terrains from coarse resolution data can be seen in the marked areas in Figure 3, Figure 4, Figure 5, and Figure 6.

The comparison of the surfaces of the resulting DEMs using profiles in the locations showed in Figure 8 reveals a clearer advantage of the Kriging interpolation method over the original coarse resolution DEM and the DEMs created by

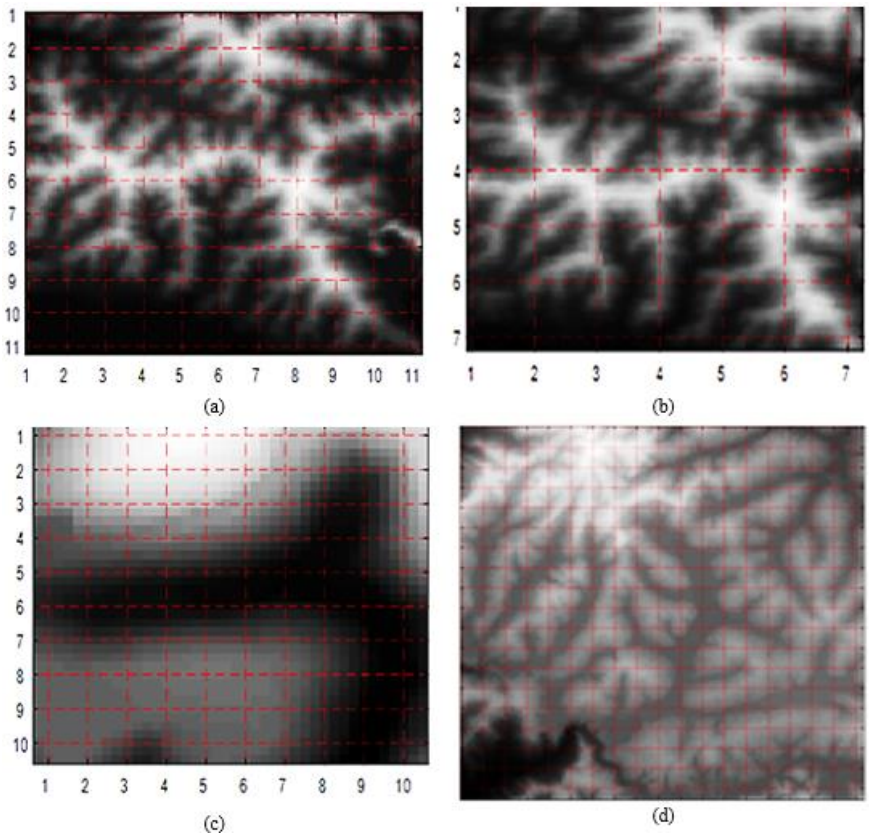

Figure 7. The positions of profiles for DEM accuracy evaluation: (a) Nghe An 20m dataset; (b) Nghe An 30m dataset; (c) Lang Son 5m dataset; and (d) Dac Ha 30m dataset.

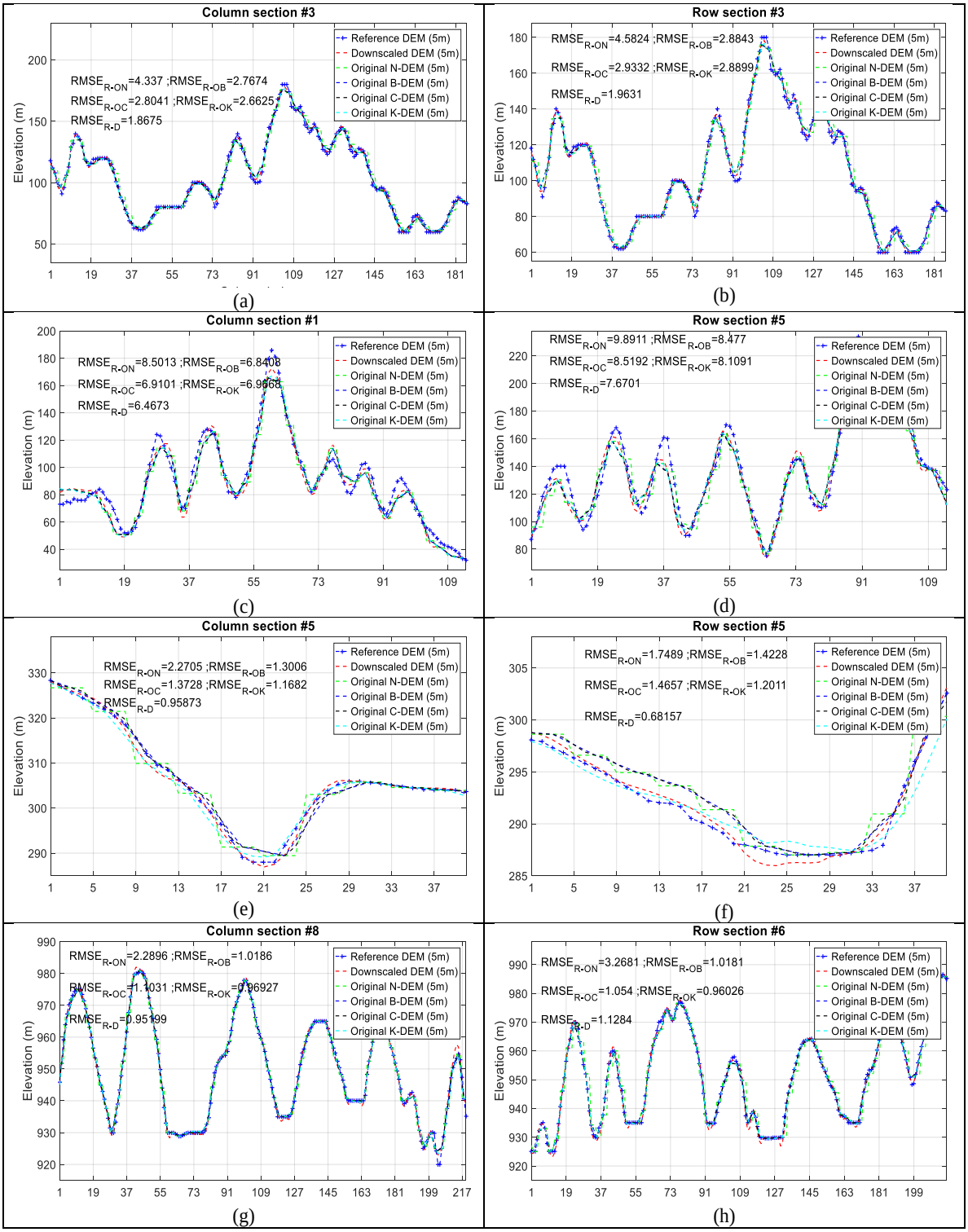

Figure 8. Comparison of reference surface (reference DEM), original coarse resolution surface (original N-DEM), bilinear (original B-DEM) and bi-cubic (original C-DEM) resampled surfaces based on profiles: (a) a column profile for 20 m degraded dataset in Nghe An; (b) a column profile for 30 m degraded dataset in Nghe An, (c) a column profile for 5 m sampled dataset in Lang Son; (d) a column profile for 30 m sampled dataset in Dac Ha; (e) a row profile for 20 m degraded dataset in Nghe An; (f) a row profile for 30 m degraded dataset in Nghe An; (g) a row profile for 5 m sampled Lang Son dataset; a row profiles for 30 m sampled dataset in Dac Ha, Vietnam.

resampling methods. In Figure 8, the elevation profiles of the Kriging interpolated DEMs are closer to the profiles of reference DEMs than those of the bilinear and bi-cubic resampled for both degraded and sampled datasets.This is most clearly seen in the 5 m Lang Son dataset in Figure 8(e) (a column profile) and Figure 8(f) (a row profile) in places such as tops of hills or bottoms of valleys. In these images, it is possible to observe that the surfaces from the bilinear and bi-cubic resampling methods are closer to the original coarse spatial resolution surface while the surface formed by the Kriging interpolation DEM are closer to the 5 m reference surface. The Kriging interpolation performed much more accurately than the bilinear and bi-cubic resampling methods for more extreme elevation features such as the tops of ridges and hills or bottoms of valleys, especially for V-shaped valleys and sharp ridges and hills.

The visual comparison of scatterplots in Figure 9, Figure 10, Figure 11, and Figure 12 also showed the better matchbetweenthe results of the resampling methods and the reference DEM data in comparison with the original coarse DEM. In these scatterplots, the two DEM data are considered to be closer if the data points are located closer to the regression line. That means the slope coefficient m is closer to the value of 1 and the intercept coefficient b is closer to the value of 0.

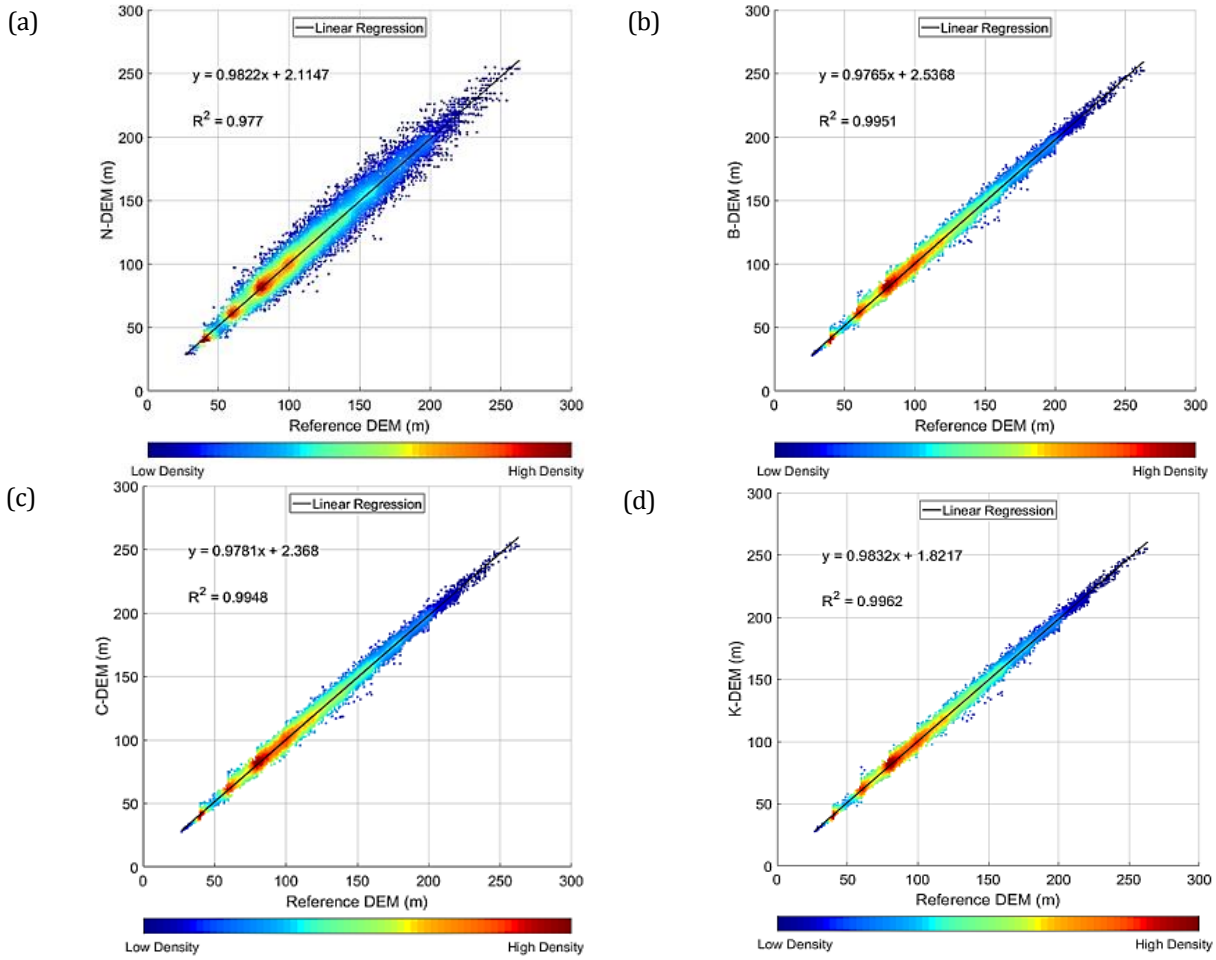

Figure 9. Scatterplots of the reference fine spatial resolution DEM against the downscaled DEM for the degraded 20 m NgheAn dataset test: (a) reference DEM and coarse degraded DEM (N-DEM), (b) the reference DEM and the bilinear resampled DEM (B-DEM), (c) the reference DEM and the bi-cubic resampled DEM (C-DEM), (d) the reference DEM and Kriging interpolated DEM (K-DEM).

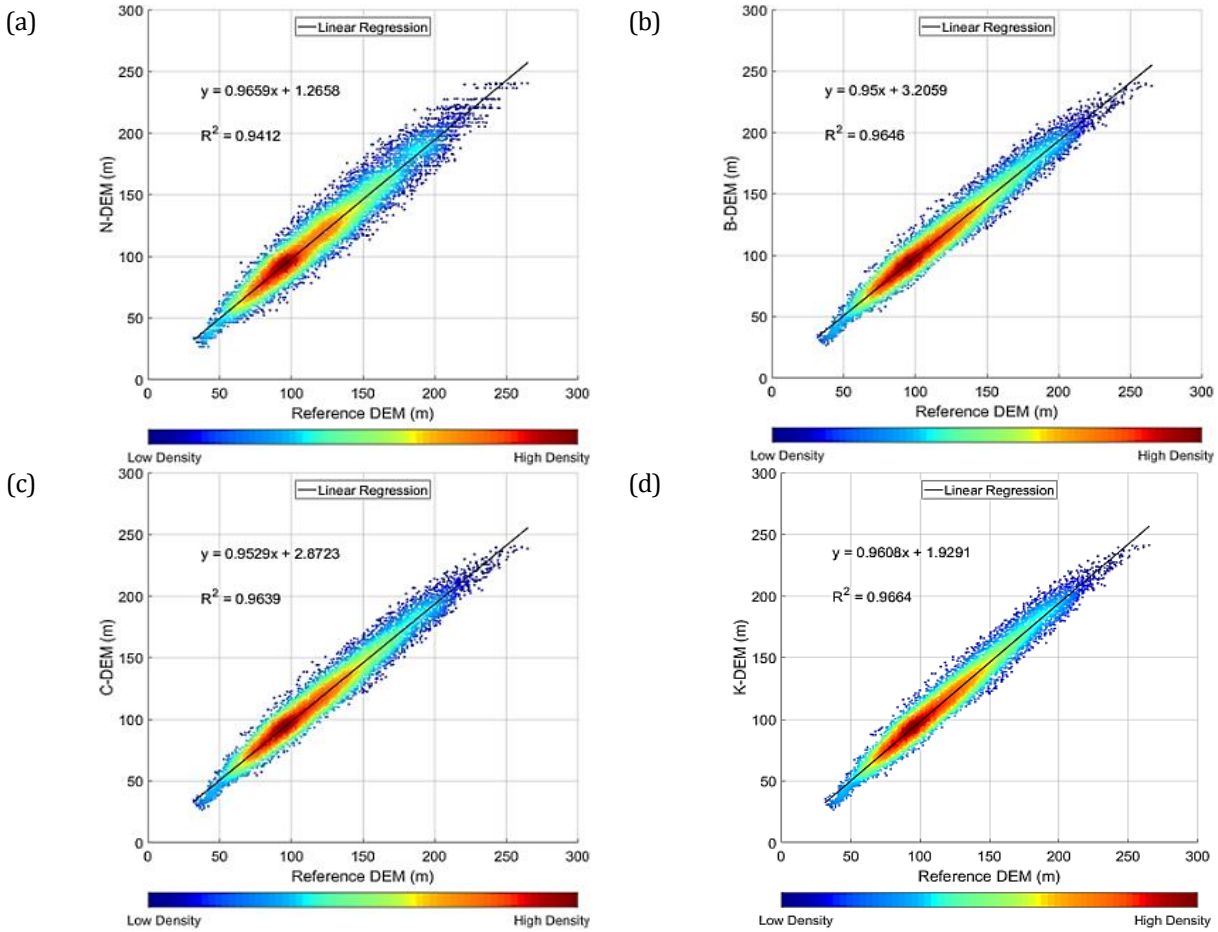

Figure 10. Scatterplots of the reference fine spatial resolution DEM against the downscaled DEMs for the degraded 30 m Nghe An dataset test: (a) the reference DEM and the coarse degraded DEM (N-DEM), (b) the reference DEM and the bilinear resampled DEM (B-DEM), (c) the reference DEM and the bi-cubic resampled DEM (C-DEM), (d) the reference DEM and Kriging interpolated DEM (K-DEM).

The scatterplots of the resampling results in Figure 9, Figure 10, Figure 11, and Figure 12 showed a closer match between the reference DEM and the resampling DEMs data in comparison with the original coarse DEM data (Figure 9(a), Figure 10(a), Figure 11(a), and Figure 12(a)) and the bilinear (Figure 9(b), Figure 10(b), Figure 11(b), and Figure 12(b)), bi-cubic (Figure 9(c), Figure 10(c), Figure 11(c), and Figure 12(c)) resampling, Kriging interpolation (Figure 9(d), Figure 10(d), Figure 11(d), and Figure 12(d)) DEM data. This improvement can be seen most clearly with the 5 m sampled Lang Son and 20 m degraded Nghe An datasets. The data points in the scatterplots in Figure 9 and Figure 11 showed that it is very close to and (sometime exactly on) the best fit line and the best fit line's coefficients in these scatterplots are closer to the value of 1 and 0. Comparing the four datasets, the data points in the scatterplots in Figure 9(b), Figure 10(b), Figure 11(b) and Figure 12(b) (bilinear resampled DEM), Figure 9(c), Figure 10(c), Figure 11(c), and Figure 12(c) (bi-cubic resampled DEM, and Figure 9(d), Figure 10(d), Figure 11(d), and Figure 12(d) (Kriging interpolated DEM) are less scattered away from the best fit line than those of the original DEMs.

5. Quantitative assessment

Coinciding with the result of visual observation, quantitative assessment based on the RMSE (Table 2, Table 3, Table 4, and Table 5) reveals a greater accuracy for the resampling and Kriging interpolation methods for all four datasets. Among the two degraded data, the increase in accuracy is higher for 20 m data.

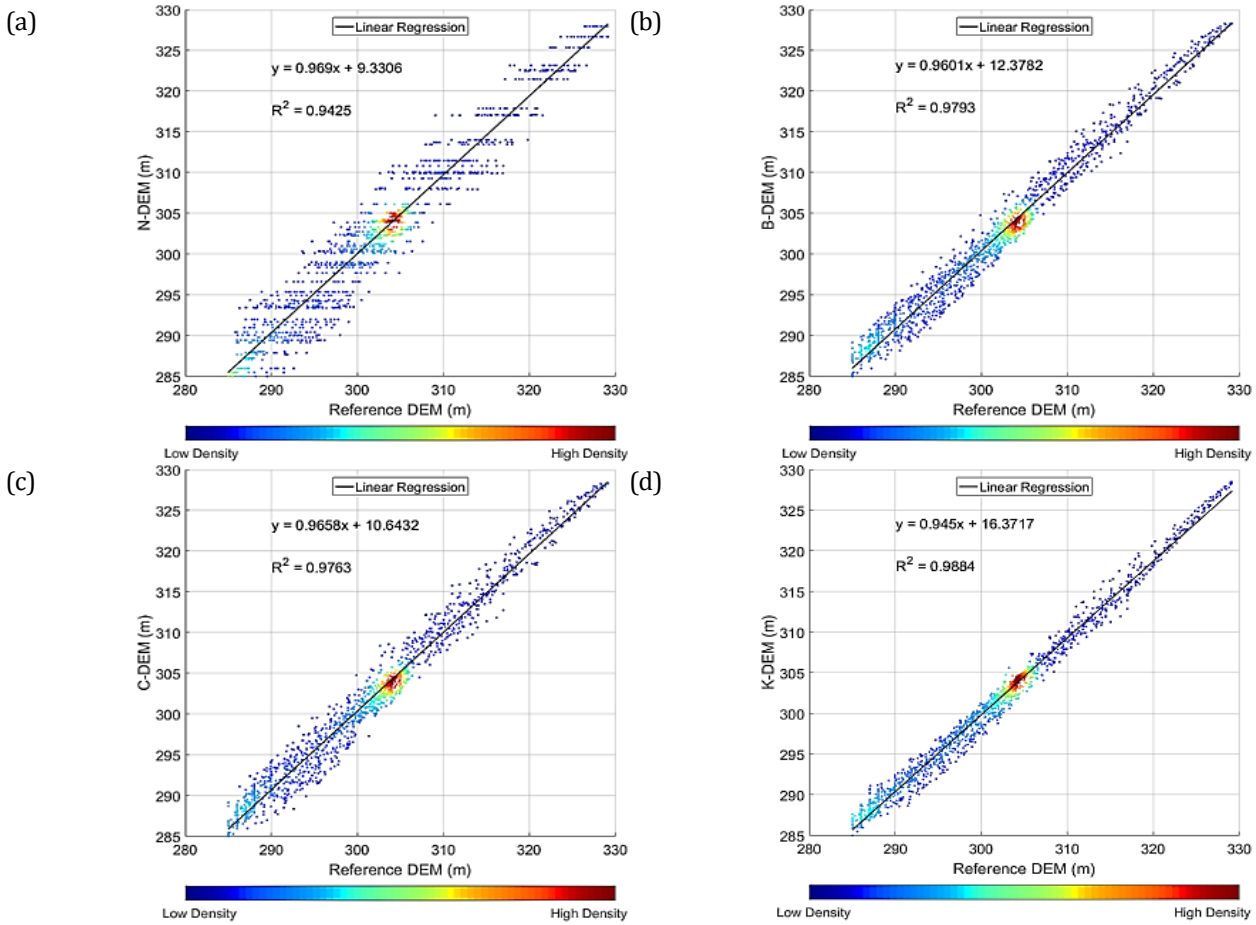

Figure 11. Scatterplots of the reference fine spatial resolution DEM against the downscaled DEM for the sampled 5 m Lang Son dataset test: (a) the reference DEM and coarse degraded DEM (N-DEM), (b) the reference DEM and the bilinear resampled DEM (B-DEM), (c) the reference DEM and the bi-cubic resampled DEM (C-DEM), (d) the reference DEM and Kriging interpolated DEM (K-DEM).

The RMSEs for the bilinear, bi-cubic resampling and Kriging interpolation methods are 3.3716 m, 3.3716 m and 2.8874 m, respectively. Comparing with the RMSE of the original 60 m data, the RMSE of the resampled DEMs at 20 m reduced significantly for all three methods. For the Nghe An 30 m degraded test data, the increase in accuracy for resampling algorithms is not as large as for the 20 m datasets but it is still very convincing with the RMSE decreased by around 20% comparing with the original 90 m DEM. Similar to that of the degraded datasets, the accuracy for sampled datasets also increased considerably. The RMSE of 5 m Lang Son data decreased sharply for the resampling algorithms DEM with the values of 1.5139 m for bilinear, 1.6 m for bi-cubic resampling, and 1.2092 m for the Kriging interpolation. The result for 30 m Dac Ha test is not as impressive as that of 5 m Lang Son data, however, the improvement of DEM accuracy is still significant with the RMSE decreased by around 50% in comparison with the original coarse images. These statistics demonstrate that the resampling methods can increase the accuracy of the gridded DEM when it is used to downscale DEM to a finer spatial resolution.

The increase in accuracy in term of RMSE for the profiles demonstrated the effects of the terrain features on the algorithm. For the 20 m and 30 m datasets in Nghe An, the increase in accuracy between the original and resampled DEMs was relatively constant. For the 30 m dataset, the increase in accuracy for most profiles was between 20% and for the 5 m sampled Lang Son dataset is more variable with the smallest

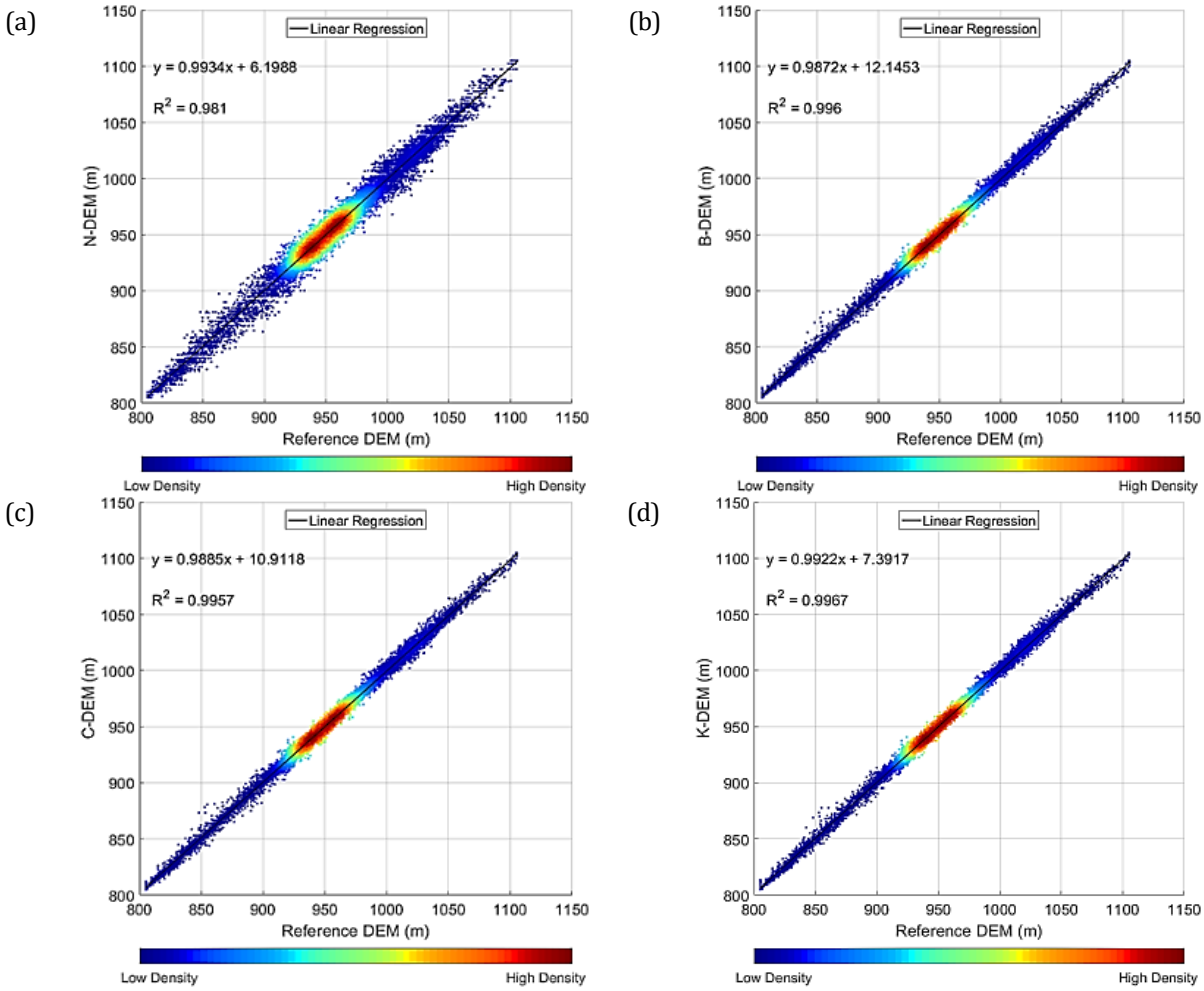

Figure 12. Scatterplots of the reference fine spatial resolution DEM against the downscaled DEM for the sampled 30 m Dac Ha dataset test: (a) the reference DEM and the coarse degraded DEM (N-DEM), (b) the reference DEM and the bilinear resampled DEM (B-DEM), (c) the reference DEM and the bi-cubic resampled DEM (C-DEM), (d) the reference DEM and Kriging interpolated DEM (K-DEM).

value of 18% and the largest value of 60%. This is because most of the profiles with a large increase in accuracy of more than 65% (such as column cross-sections 2, 4 and row cross-sections 2, 4, 9) are located in areas of specific terrain such as valley bottoms or the tops of hills. In contrast, the profiles with a smaller increase in accuracy occur mostly on the sides of mountains where the surface of the original (coarse) DEM is relatively close to the reference (fine) DEM. The smaller amount of variation in the accuracy increasing for the 20 m and 30 m degraded datasets and 30 m sampled Dac Ha dataset occurs because most profiles located along many different types of terrain rather than occurring mostly on specific terrain forms. The range of the increase in accuracy for the 20 m dataset is 20% and between 50% and 70%.The similarity of the two DEMs can also be evaluated quantitatively using the linear regression coefficients (m, b) and the correlation coefficient R. Comparing two DEMs, if the elevation of a pixel in the reference dataset is x and the elevation of the corresponding pixel in the comparing dataset is y, the expected perfect fit line should be $y = x$ such that $m = 1$ and $b = 0$. Because the value of m may be greater or smaller than 1 and the value of b may be greater or smaller than 0, comparison between different values of m and b to define the closeness of them to 1 and 0, respectively, sometimes it is not easy to evaluate. To make it easier for this evaluation, the sub-parameters such as $|1 - m|$ and $|b|$ were.

Table 2 Root mean squared error (RMSE) for the predictions using the bilinear resampling, bi-cubic resampling and the Kriging algorithms for the Nghe An 20 m DEM (CP stands for Column Profile, RP stands for Row Profile.)

Datasets	Original coarse DEM RMSE (m)	Bilinear Resampling RMSE (m)	Accuracy improvement over coarse DEM (%)	Bi-cubic Resampling RMSE (m)	Accuracy improvement over coarse DEM	Kriging interpolation RMSE (m)	Accuracy improvement over coarse DEM
Overall RMSE	6.9326	3.3026	52.4%	3.3716	51.4%	2.8874	58.4%
CP 1*	4.5389	3.0986	31.7%	3.1431	30.8%	3.2242	29.0%
CP 2	4.4169	2.8131	36.3%	2.8973	34.4%	2.8798	34.8%
CP 3	4.3370	2.7674	36.2%	2.8041	35.3%	2.6625	38.6%
CP 4	4.4689	2.9057	35.0%	2.9731	33.5%	2.7696	38.0%
CP 5	4.0911	2.9148	28.8%	2.9445	28.0%	2.9336	28.3%
CP 6	3.8029	2.5245	33.6%	2.5619	32.6%	2.6330	30.8%
CP 7	4.6677	3.1959	31.5%	3.2344	30.7%	3.1115	33.3%
CP 8	4.8884	2.9958	38.7%	3.0833	36.9%	2.9249	40.2%
CP 9	5.1846	2.9851	42.4%	3.0731	40.7%	2.7065	47.8%
CP 10	5.2172	3.3379	36.0%	3.4256	34.3%	3.2270	38.1%
CP 11	4.3794	2.5489	41.8%	2.6209	40.2%	2.4393	44.3%
RP 1	6.9375	3.7005	46.7%	3.6816	46.9%	3.6813	46.9%
RP 2	6.4972	2.9903	54.0%	3.0293	53.4%	2.8799	55.7%
RP 3	4.5824	2.8843	37.1%	2.9332	36.0%	2.8899	36.9%
RP 4	7.0182	3.4087	51.4%	3.4013	51.5%	3.1660	54.9%
RP 5	6.5620	3.5779	45.5%	3.5906	45.3%	3.4508	47.4%
RP 6	6.9686	3.3586	51.8%	3.4280	50.8%	3.3106	52.5%
RP 7	6.8329	3.1977	53.2%	3.2778	52.0%	3.1780	53.5%
RP 8	7.7733	3.7850	51.3%	3.7997	51.1%	3.7522	51.7%
RP 9	5.7281	2.7969	51.2%	2.9109	49.2%	2.7287	52.4%
RP 10	5.0358	2.3813	52.7%	2.4803	50.7%	2.2053	56.2%
RP 11	2.3477	1.3837	41.1%	1.4051	40.1%	1.3916	40.7%

Table 3. Root mean squared error (RMSE) for the predictions using the bilinear resampling, bi-cubic resampling and the Kriging algorithms for the NgheAn SRTM 30 m DEM.

Datasets	Original coarse DEM RMSE (m)	Bilinear Resampling RMSE (m)	Accuracy improvement over coarse KDEM (%)	Bi-cubic Resampling RMSE (m)	Accuracy improvement over coarse DEM (%)	Kriging resampling RMSE (m)	Accuracy improvement over coarse DEM (%)
Overall RMSE	11.1379	8.8105	20.9%	8.8736	20.3%	8.5719	23.0%
CP 1	8.5013	6.8408	19.5%	6.9101	18.7%	6.9668	18.1%
CP 2	9.7106	8.4326	13.2%	8.4863	12.6%	8.5101	12.4%
CP 3	11.6961	10.7635	8.0%	10.8141	7.5%	11.0702	5.4%
CP4	10.0198	8.9907	10.3%	9.0225	10.0%	9.2379	7.8%
CP 5	9.2745	7.0420	24.1%	7.2130	22.2%	7.3050	21.2%
CP 6	11.5945	9.8018	15.5%	9.8618	14.9%	9.7752	15.7%
CP 7	9.7925	8.3543	14.7%	8.4407	13.8%	8.4730	13.5%
RP 1	10.4429	9.8024	6.1%	9.8357	5.8%	9.6199	7.9%
RP 2	9.9168	8.0953	18.4%	8.0897	18.4%	8.0478	18.8%
RP 3	10.5144	9.6251	8.5%	9.6645	8.1%	9.5933	8.8%
RP 4	9.9849	7.7341	22.5%	7.8310	21.6%	7.6501	23.4%
RP 5	9.8911	8.4770	14.3%	8.5192	13.9%	8.1091	18.0%
RP 6	8.8079	7.7367	12.2%	7.7801	11.7%	7.3437	16.6%
RP 7	6.6352	6.4032	3.5%	6.4005	3.5%	6.2829	5.3%

Table 4. Root mean squared error (RMSE) for the predictions using the bilinear resampling, bi-cubic resampling and the Kriging algorithms for the Lang Son 5 m DEM.

Datasets	Original coarse DEM RMSE (m)	Bilinear Resampling RMSE (m)	Accuracy improvement over coarse DEM	Bi-cubic Resampling RMSE (m)	Accuracy improvement over coarse DEM	Kriging interpolation RMSE (m)	Accuracy improvement over coarse DEM
Overall RMSE	2.4571	1.5139	38.4%	1.6000	34.9%	1.2092	50.8%
CP 1	1.4960	1.2419	17.0%	1.2912	13.7%	0.8727	41.7%
CP2	1.6962	1.1635	31.4%	1.1821	30.3%	1.1771	30.6%
CP 3	2.0641	1.4043	32.0%	1.4791	28.3%	1.1067	46.4%
CP 4	2.2345	1.3591	39.2%	1.4586	34.7%	0.9983	55.3%
CP 5	2.2705	1.3006	42.7%	1.3728	39.5%	1.1682	48.5%
CP 6	2.3084	1.7034	26.2%	1.7805	22.9%	0.9444	59.1%
CP 7	2.0349	1.6198	20.4%	1.6569	18.6%	0.9789	51.9%
CP 8	2.0325	1.4749	27.4%	1.5564	23.4%	0.8047	60.4%
CP 9	2.0937	1.2861	38.6%	1.3578	35.1%	1.5940	23.9%
CP 10	1.9876	1.2374	37.7%	1.2959	34.8%	1.7913	9.9%
RP 1	1.9569	1.4024	28.3%	1.4348	26.7%	0.9771	50.1%
RP 2	2.2873	1.6555	27.6%	1.7196	24.8%	1.5087	34.0%
RP 3	2.3612	1.6712	29.2%	1.7451	26.1%	1.2566	46.8%
RP 4	1.9510	1.4361	26.4%	1.5174	22.2%	1.6807	13.9%
RP 5	1.7489	1.4228	18.6%	1.4657	16.2%	1.2011	31.3%
RP 6	1.7289	1.4081	18.6%	1.4297	17.3%	1.4138	18.2%
RP 7	1.6217	1.1567	28.7%	1.2101	25.4%	0.7408	54.3%
RP 8	1.3897	0.8887	36.1%	0.9730	30.0%	0.5217	62.5%
RP 9	1.4791	0.9317	37.0%	0.9592	35.1%	0.7389	50.0%
RP 10	1.8042	1.4126	21.7%	1.4593	19.1%	0.9341	48.2%

calculated (Table 6). Accordingly, the smaller values of $|1 - m|$ and $|b|$ simultaneously are, the more similar the two datasets are. The third parameter for evaluating the fitting of the two datasets is the correlation coefficient *R*. The correlation coefficient measures the association between two datasets and, thus, captures the distribution of the data points in the scatterplots around the best fit line. The closer value of R^2 to 1, the more data points are located close to the best fit line. A perfect match between two DEM datasets means that all the data points are located on the identity line ($y = x$) and the coefficient of determination $R^2 = 1$. That means the two datasets are exactly the same if the value of *m* is equal to 1, *b* is equal to 0 and R^2 is equal to 1, simultaneously

To evaluate the results of the different methods, linear regression models were fitted to the relation between the reference data and resampled data (Table 6). The coefficient values show the better fitting of the Kriging interpolated DEMs with the reference DEMs than those of the original DEMs, bilinear and bi-cubic resampled DEMs. For all four datasets, the values of parameters *m*, *b* and R^2 of Kriging interpolated DEMs are closer to the values of 1, 0, and 1, respectively, than those of the original, bilinear and bi-cubic resampled DEMs. In case of the Lang Son 5 m resampled dataset, the values $|1 - m| = 0.0550, |b| = 16.3717$ and $R^2 = 0.9884$ for the Kriging interpolated DEM showed greater similarity to the reference DEM than those of the original coarse DEM ($|1 - m|$ = 0.0310, $|b|$ = 9.3306 and R^2 = 0.9425), bilinear resampled DEM ($|1 - m|$ = 0.0399, $|b|$ = 12.3782 and R^2 = 0.9793), bi-cubic resampled DEM ($|1 - m|$ = 0.0342, $|b|$ = 10.6432 and R^2 = 0.9763. Linear regression statistics for the Dac Ha sampled data also showed the better matching of the Kriging interpolation DEM to the reference with $|1 - m|$ = 0.0078, $|b|$ = 7.3917 and R^2 = 0.9967 comparing with $|1 - m|$ = 0.0128, $|b|$ = 12.1453 and R^2 = 0.9960 for bilinear resampling, $|1 - m|$ = 0.0115, $|b|$ = 10.9118 and R^2 = 0.9959 for bi-cubic resampling. Among three resampling methods, the most inaccurate results are from the bi-cubic but comparing with the

original coarse resolution data, these results were much more accurate.

Linear regression coefficients for the 20 m Nghe An degraded dataset showed that the resampled DEM matches closely to the reference DEM. Surprisingly, the comparison also showed that the original coarse DEM with parameters of $|1 - m|$ = 0.0178 and $|b|$ = 2.1147 is generally more matched (less bias) to the reference DEM than the resampled DEMs with $|1 - m|$ = 0.0235 and $|b|$ = 2.5368, and $|1 - m|$ = 0.0219 and $|b|$ = 2.3680 for bilinear and bi-cubic resampled DEMs, respectively. However, more data points of the bilinear (R^2 = 0.9951) and bi-cubic (R^2 = 0.9948) resampled DEMs are distributed close to the best fit line than those of the original 20 m DEM (R^2 = 0.9770).For the 30 m degraded dataset, the increase in prediction precision of the resampled methods is clearly seen when comparing the linear regression parameters of the three methods.

Comparing the slope parameter m and intercept parameter b of the best fit lines of all four datasets, it is clear that all the slope parameters m of the resampled DEMs are smaller than 1 and the intercept parameters b are larger than 0. This means that for locally-low places (usually the bottom of valleys) the pixels of the DEM data produced by these methods are likely to be higher than the corresponding pixels in the reference DEM. Conversely, for locally-high places such as the top of hills or mountain ridges, the elevation of the pixels in the resampled DEM data is likely lower than that of the corresponding pixels in the reference image. This is due to the smoothing effect (referred to as conditional bias where highs are under-predicted and lows are over-predicted).

6. Conclusion

A test for resampling algorithms to increase the spatial resolution and accuracy of gridded DEMs was implemented and demonstrated comprehensively using data with different DEM spatial resolutions and characteristics. Tests of there sampling algorithms were implemented on two types of elevation datasets; degraded DEMs at 20 m and 30 m spatial resolution in Nghe An

Table 5. Root mean squared error (RMSE) for the predictions using the bilinear resampling, bi-cubic resampling and the Kriging algorithms for the DacHa 30 m DEM.

Datasets	Original coarse DEM RMSE (m)	Bilinear Resampling RMSE (m)	Accuracy improvement over coarse DEM	Bi-cubic Resampling RMSE (m)	Accuracy improvement over coarse DEM	Kriging interpolation RMSE (m)	Accuracy improvement over coarse DEM
Overall RMSE	5.0680	2.3284	54.1%	2.4218	52.2%	2.1095	58.4%
CP 1	4.0702	2.3434	42.4%	2.4436	40.0%	2.2330	45.1%
CP 2	4.0203	2.0594	48.8%	2.2048	45.2%	1.9960	50.4%
CP 3	3.8541	2.0370	47.1%	2.0956	45.6%	2.1132	45.2%
CP 4	3.5399	2.2395	36.7%	2.2698	35.9%	2.1836	38.3%
CP 5	3.4595	1.8231	47.3%	1.9178	44.6%	1.7027	50.8%
CP 6	2.3885	1.3172	44.9%	1.3603	43.0%	1.3345	44.1%
CP 7	2.6743	1.1377	57.5%	1.2514	53.2%	1.0253	61.7%
CP 8	2.2896	1.0186	55.5%	1.1031	51.8%	0.9693	57.7%
CP 9	2.0938	1.0068	51.9%	1.0624	49.3%	0.9942	52.5%
RP 1	4.6476	1.8714	59.7%	1.9762	57.5%	2.0200	56.5%
RP 2	4.6907	2.2973	51.0%	2.3739	49.4%	2.2684	51.6%
RP 3	4.5113	1.7205	61.9%	1.8051	60.0%	1.4827	67.1%
RP 4	3.6187	1.4932	58.7%	1.5675	56.7%	1.3472	62.8%
RP 5	3.9713	1.2816	67.7%	1.4015	64.7%	1.1203	71.8%
RP 6	3.2681	1.0181	68.8%	1.0540	67.7%	0.9603	70.6%
RP 7	2.8494	1.5355	46.1%	1.5676	45.0%	1.3829	51.5%
RP 8	3.0366	1.0666	64.9%	1.0934	64.0%	1.1003	63.8%
RP 9	4.2630	1.9581	54.1%	2.0194	52.6%	1.8029	57.7%
RP 10	5.2869	2.3473	55.6%	2.4070	54.5%	2.5440	51.9%

Table 6. Linear regression coefficients for 20 m Nghe An and 30 m Nghe An resampled datasets, and the Lang Son 5 m and Dac Ha 30 m sampled datasets.

Datasets		Linear Regression Coefficients				
		m	$\|1-m\|$	b	$\|b\|$	R^2
20 m Nghe An dataset	60 m degraded DEM	0.9822	0.0178	2.1147	2.1147	0.9770
	20 m bilinear resampled DEM	0.9765	0.0235	2.5368	2.5368	0.9951
	20 m bi-cubic resampled DEM	0.9781	0.0219	2.3680	2.3680	0.9948
	20 m Kriging interpolated DEM	0.9832	0.0168	1.8217	1.8217	0.9962
30 m Nghe An dataset	90 m degraded DEM	0.9659	0.0341	1.2658	1.2658	0.9412
	30 m bilinear resampled DEM	0.9500	0.0500	3.2057	3.2057	0.9646
	30 m bi-cubic resampled DEM	0.9529	0.0471	2.8723	2.8723	0.9639
	30 m Kriging interpolated DEM	0.9608	0.0392	1.9291	1.9291	0.9964
Lang Son dataset	20 m coarse DEM	0.9690	0.0310	9.3306	9.3306	0.9425
	5 m bilinear resampled DEM	0.9601	0.0399	12.3782	12.3782	0.9793
	5 m bi-cubic resampled DEM	0.9658	0.0342	10.6432	10.6432	0.9763
	5 m Kriging interpolated DEM	0.9450	0.0550	16.3717	16.3717	0.9884
Dac Ha dataset	90 m coarse DEM	0.9934	0.0066	6.1988	6.1988	0.9810
	30 m bilinear resampled DEM	0.9872	0.0128	12.1453	12.1453	0.9960
	30 m bi-cubic resampled DEM	0.9885	0.0115	10.9118	10.9118	0.9959
	30 m Kriging interpolated DEM	0.9922	0.0078	7.3917	7.3917	0.9967

province, Vietnam, and sampled DEMs at 5m spatial resolution in Lang Son province (from ground surveying elevation data), and 30 m spatial resolution in Dac Ha, Kontum Province, Vietnam (generated from the contour lines).

The test results revealed a considerable increase in accuracy for the Kriging interpolated gridded DEMs in comparison with the original (coarse) gridded DEM, and the bilinear and bi-cubic resampling. Visual assessment revealed the greater similarity of the Kriging interpolated DEMs with the reference DEM than the DEMs generated by bilinear and bi-cubic resampling methods. Quantitative accuracy assessment based on the RMSE revealed an increase in DEM accuracy for the Kriging algorithm over the bilinear and bi-cubic resampling methods. The RMSE of the Kriging interpolated DEMs decreased by approximately 58%, 23%, 50%, and 58% for the 20 m and 30 m degraded DEMs in Nghe An province, 5 m sampled DEM in Lang son province, and 30 m sampled DEM in Dac Ha, Vietnam, respectively.

Further evaluation was also implemented using linear regression of the original fine spatial resolution DEM against the original, the bilinear and bi-cubic resampled, and Kriging interpolated DEMs, particularly focusing on the coefficients m, b and R^2. Analysis of these parameters showed that the Kriging interpolated DEMs was closer to the reference DEMs than the original DEM and those produced using the bilinear and bi-cubic resampling methods.

Tài liệu tham khảo

Alganci, U., Besol, B., Sertel, E., 2018. Accuracy Assessment of Different Digital Surface Models. ISPRS Int. J. *Geo-Information* 7, 114. https://doi.org/10.3390/ijgi7030114

ASPRS, 2015. ASPRS Positional Accuracy Standards for Digital Geospatial Data. Photogramm. Eng. *Remote Sens. 81*. https://doi.org/10.14358/PERS.81.3.A1-A26

Band, L.E., Moore, I.D., 1995. Scale: Landscape attributes and geographical information systems. Hydrol. *Process. 9*, 401–422. https://doi.org/10.1002/hyp.3360090312

Bian, L., Butler, R., 1999. Comparing Effects of Aggregation Methods on Statistical and Spatial Properties of Simulated Spatial Data. Photogramm. Eng. *Remote Sens*.

Bolstad, Paul V. & Stowe, T., 1994. An Evaluation Accuracy : of DEM Elevation , Slope , and

Aspect. ISPRS J. Photogrametric Eng. *Remote Sens 60*, 1327-1332.

Chang, K., Tsai, B., 2008. The Effect of DEM Resolution on Slope and Aspect Mapping. *Cartogr. Geogr. Inf. Syst. 18*, 69–77. https://doi.org/10.1559/152304091783805626

Chaubey, I., Cotter, A.S., Costello, T.A., Soerens, T.S., 2005. Effect of DEM data resolution on SWAT output uncertainty. *Hydrol. Process. 19*, 621–628. https://doi.org/10.1002/hyp.5607

Dixon, B., Earls, J., 2009. Resample or not?! Effects of resolution of DEMs in watershed modeling. *Hydrol. Process*. https://doi.org/10.1002/hyp.7306

Fadnavis, S., 2014. Image Interpolation Techniques in Digital Image Processing : An Overview. *Int. J. Eng. Res*. Appl. 4, 70–73.

Grohmann, C.H., Steiner, S.S., 2008. SRTM resample with short distance-low nugget kriging. Int. J. *Geogr. Inf. Sci. 22*, 895–906. https://doi.org/10.1080/13658810701730152.

Guo, Q., Li, W., Yu, H., Alvarez, O., 2013. Effects of Topographic Variability and Lidar Sampling Density on Several DEM Interpolation Methods. Photogramm. Eng. Remote Sens. 76, 701–712. https://doi.org/10.14358/pers.76.6.701.

Kidner, D., Dorey, M., Smith, D., 1999. What's the point? Interpolation and extrapolation with a regular grid DEM, in: GeoComputation.Org.

Kienzle, S., 2003. The Effect of DEM Raster Resolution on First Order, Second Order and Compound Terrain Derivatives. Trans. GIS 8, 83–111. https://doi.org/10.1111/j.1467-9671.2004.00169.x

Kuo, W.L., Steenhuis, T.S., McCulloch, C.E., Mohler, C.L., Weinstein, D.A., DeGloria, S.D., Swaney, D.P., 1999. Effect of grid size on runoff and soil moisture for a variable-source-area hydrology model. *Water Resour. Res. 35*, 3419–3428. https://doi.org/10.1029/1999WR900183

Li, J., Wong, D.W.S., 2010. Effects of DEM sources on hydrologic applications. Comput. *Environ. Urban Syst. 34*, 251-261. https://doi.org/10.1016/j.compenvurbsys.2009.11.002

Liu, X., 2008. Airborne LiDAR for DEM generation: Some critical issues. *Prog. Phys. Geogr*. https://doi.org/10.1177/0309133308089496

Rapinel, S., Hubert-Moy, L., Clément, B., Nabucet, J., Cudennec, C., 2015. Ditch network extraction and hydrogeomorphological characterization using LiDAR-derived DTM in wetlands. *Hydrol. Res*. https://doi.org/10.2166/nh.2013.121

Rawat, K.S., Krishna, G., Mishra, A., Singh, J., Mishra, S.V., 2018. Effect of DEM data resolution on low relief region sub-watershed boundaries delineating using of SWAT model and DEM derived from CARTOSAT-1 (IRS-P5), SRTM and ASTER. *J. Appl. Nat. Sci.* 6. https://doi.org/10.31018/jans.v6i1.391

Reddy, A.S., Reddy, M.J., 2015. Evaluating the influence of spatial resolutions of DEM on watershed runoff and sediment yield using SWAT. J. Earth Syst. Sci. 124, 1517–1529. https://doi.org/10.1007/s12040-015-0617-2

Rees, W.G., 2000. The accuracy of Digital Elevation Models interpolated to higher resolutions. Int. J. Remote Sens. 21, 7–20. https://doi.org/10.1080/014311600210957

Saksena, S., Merwade, V., 2015. Incorporating the effect of DEM resolution and accuracy for improved flood inundation mapping. J. Hydrol. 530, 180–194. https://doi.org/10.1016/J.JHYDROL.2015.09.069

Schoorl, J. M., Sonneveld, M. P. W., Veldkamp, A., 2000. Three-dimensional landscape process modelling: The effect of DEM resolution. *Earth Surf. Process. Landforms*. https://doi.org/10.1002/1096-9837(200008)25:9<1025::AID-ESP116>3.0.CO;2-Z

Shi, W., Wang, B., Tian, Y., 2014. Accuracy Analysis of Digital Elevation Model Relating to Spatial Resolution and Terrain Slope by Bilinear Interpolation. *Math. Geosci. 46*, 445–481. https://doi.org/10.1007/s11004-013-9508-8

Smith, M. P., Zhu, A. X., Burt, J. E., Stiles, C., 2006. The effects of DEM resolution and neighborhood size on digital soil survey.

Geoderma 137, 58–69. https://doi.org/10.1016/j.geoderma.2006 .07.002

Sulis, M., Paniconi, C., Camporese, M., 2011. Impact of grid resolution on the integrated and distributed response of a coupled surface-subsurface hydrological model for the des Anglais catchment, Quebec. Hydrol. *Process. 25*, 1853 - 1865. https://doi.org/10.1002/hyp.7941

Vázquez, R. F., Feyen, J., 2007. Assessment of the effects of DEM gridding on the predictions of basin runoff using MIKE SHE and a modelling resolution of 600 m. J. Hydrol 334, 73-87. https://doi.org/10.1016/j.jhydrol.2006.10.001

Vieux, B. E., 2006. DEM Aggregation and Smoothing Effects on Surface Runoff Modeling. J. Comput. *Civ. Eng 7*. https://doi.org/10.1061/(asce)0887-3801(1993)7:3(310)

Whitehead, K., Hugenholtz, C. H., 2015. Applying ASPRS Accuracy Standards to Surveys from Small Unmanned Aircraft Systems (UAS). Photogramm. Eng. *Remote Sens 81*, 787–793. https://doi.org/10.14358/pers.81.10.787

Wilson, J. P., 2012. Digital terrain modeling. *Geomorphology 137*, 107-121. https://doi.org/10.1016/j.geomorph.2011.03.012

Wu, S., Li, J., Huang, G. H., 2008. A study on DEM-derived primary topographic attributes for hydrologic applications: Sensitivity to elevation data resolution. *Appl. Geogr*. https://doi.org/10.1016/j.apgeog.2008.02.006

Zhao, Z., Benoy, G., Chow, T. L., Rees, H. W., Daigle, J. L., Meng, F. R., 2010. Impacts of accuracy and resolution of conventional and LiDAR based DEMs on parameters used in hydrologic modeling. *Water Resour. Manag* 24, 1363-1380. https://doi.org/10.1007/s11269-009-9503-5.